Accident Analysis and Prevention 125 (2019) 275–289

Contents lists available at ScienceDirect

Accident Analysis and Prevention

journal homepage: www.elsevier.com/locate/aap

Impact of heterogeneity of car-following behavior on rear-end crash risk

Junjie Zhang[a,b], Yunpeng Wang[a,b], Guangquan Lu[a,b,*]

[a] Beijing Advanced Innovation Center for Big Data and Brain Computing, Beijing Key Laboratory for Cooperative Vehicle Infrastructure Systems and Safety Control, Beijing 100191, China

[b] School of Transportation Science and Engineering, Beihang University, Beijing 100191, China

ARTICLE INFO

Keywords:
Heterogeneity
Desired safety margin
Rear-end crash
Risk perception
Driving behavior parameter

ABSTRACT

An increasing number of vehicles travel on freeways result not only in traffic congestions but also accidents. Rear-end crashes in freeways can be collectively attributed to drivers, vehicles, and road infrastructure, but driving behavior plays a key role in influencing car-following safety. This study aims to investigate the impact of heterogeneity of driving behavior on rear-end crash risk. Driving behavior depends on perceived risk levels, acceleration and deceleration habits, and driver reaction characteristics. Thus, the influencing factors of rear-end crash risk were initially analyzed by using the desired safety margin (DSM) model. Subsequently, five driving behavior parameters, including upper and lower limits of DSM, sensitivity coefficients of acceleration and deceleration, and response time, were calibrated by using the vehicle trajectories from the Next Generation Simulation I-80 datasets. Simulation experiments were designed to evaluate the impact of heterogeneity of car-following behavior on rear-end crash risk. Results showed that decreasing the lower (or upper) limit of the DSM, increasing the response time, increasing the sensitivity coefficient for acceleration, or decreasing the sensitivity coefficient for deceleration can increase rear-end crash risk. In addition, if stable and unstable driving styles coexist, then their proportions have important influences on rear-end crash risk. These results imply that two critical factors affect shock waves, namely, driving behavior characteristics and proportion of different driving styles. Thus, a potential strategy for the adjustment of the proportions of unstable driving styles can attenuate shock waves and reduce rear-end crash risk to a certain extent. Moreover, a wide extent of driving behavior heterogeneity can attenuate shock waves and subsequently reduce rear-end crash risk. Overall, driving behavior heterogeneity has an important impact on rear-end crash risk. Exploring the effect of each driving behavior parameter on rear-end crash probability is useful for urban road traffic control, and it can provide improved understanding of abnormal driving behavior characteristics to minimize rear-end crash risks.

1. Introduction

In recent years, rear-end crashes on roadways have frequently occurred in China. The Traffic Management Bureau of the Ministry of Public Security of China has recorded 196,812 road traffic accidents, 211,882 injuries in traffic crashes, and 58,523 people killed due to road traffic accidents in 2014 (Huang et al., 2016). Wu and Thor (2015) and Xiao (2016) showed that rear-end accidents on China's highways accounted for approximately 40% of all traffic accidents. Thus, an analytical research on rear-end accidents should be performed to investigate the factors that contribute to and the characteristics of rear-end accidents.

In general, a transportation system comprises three elements, namely, drivers, vehicles, and road infrastructures, which all contribute to roadway crashes. A number of studies were conducted by using different modeling methods to understand the relationship between crashes and their potential causal factors (Lao et al., 2011b). Weng et al. (2014) analyzed rear-end crash risk associated with work zone operations for four different vehicle following patterns. Weng and Meng (2014) proposed a methodology to estimate rear-end crash potential of the merging vehicles traveling in the merge lane. Weng et al. (2016) proposed a method based on association rules to analyze the characteristics and contributory factors of work zone crash casualties. In addition, linear regression, Poisson regression, and negative binomial regression are widely used to study the relationship between rear-end collision and its potential causal factors. Lord and Mannering (2010) reviewed various statistical modeling techniques that can analyze collision characteristics under certain circumstances. Jovanis and Chang

* Corresponding author at: Beijing Advanced Innovation Center for Big Data and Brain Computing, Beijing Key Laboratory for Cooperative Vehicle Infrastructure Systems and Safety Control, School of Transportation Science and Engineering, Beihang University, Beijing 100191, China.
E-mail address: lugq@buaa.edu.cn (G. Lu).

https://doi.org/10.1016/j.aap.2019.02.018
Received 18 May 2018; Received in revised form 23 January 2019; Accepted 15 February 2019
Available online 23 February 2019
0001-4575/ © 2019 Elsevier Ltd. All rights reserved.

(1986) investigated related undesirable problems by using linear regression. To discuss the effect of various factors on road traffic accidents, generalized linear models, such as Poisson regression (Miaou et al., 1992; Miaou and Lum, 1993; Miaou, 1994), negative binomial regression (Poch and Mannering, 1996; Chin and Quddus, 2003; Kim et al., 2007; Geedipally et al., 2012), and other models, including random-parameter models (Anastasopoulos and Mannering, 2009; Anastasopoulos et al., 2012), Bayesian approaches (Deublein et al., 2013), and bivariate/multivariate models (Park et al., 2008; Lao et al., 2011a), were considered. Lao et al. (2014) adopted generalized linear model-based modeling principles and extended generalized nonlinear model-based approaches in rear-end crash risk analysis. Weng et al. (2015) developed a mixed probit model to describe the merging behavior, and to compute the rear-end crash risk between the merging vehicle and its neighboring vehicles using two surrogate safety measures. Weng et al. (2017) investigated the drivers' merging behavior in work zone merging areas, and proposed a time-dependent logistic regression model to provide higher prediction accuracy compared with the standard model. Weng et al. (2018) further developed a time-varying mixed logit model for the vehicle merging behavior in work zone merging areas to provide higher prediction accuracy than previous models.

Although these previous studies analyzed the relationship between rear-end collision and its potential causal factors, minimal efforts were rendered to fully explore the effect of microscale driving behavior on rear-end collision. The relationship between driving behavior and crash experience has been a long-sought research topic that is too elusive to explore. The literature also reported several attempts to correlate driving behavior with a driver's propensity to be involved in a crash. Lee (1976) presented a theory of visual control of braking in the context of car driving. It shown that the driver use visual information about visual angular velocity or time-to-collision to start braking. Wiedemann and Reiter (1992) developed psychophysical driving algorithms for the simulation model, whose car-following model consider four types of regimes where drivers adjust their desired spacing and speeds through changes in their acceleration and deceleration rates. Kim et al. (2016) explored the relationship between microscale driving behavior and crash propensity by using in-vehicle sensing devices. Driving behavior, which includes instantaneous acceleration and deceleration, driver reaction time, and risk perception, is easily affected by psychological status and environmental conditions. Recent studies have shown that driver risk perception is an important driving behavior that enables drivers to minimize collision risk in complicated traffic environments (Borowsky et al., 2012; Meir et al., 2014; Li et al., 2017).

Car following is the most common phenomenon in single lanes. The state of vehicle motion depends on a drivers' car-following behavior, and this leads to amplitude of fluctuations in vehicle speed and headway. These fluctuations lead to traffic flow instability and even crashes (Tampere et al., 2005; Tanaka et al., 2008). Hourdos (2005) argued that the occurrence of stopping shock waves causes rear-end crashes. Zheng et al. (2010) found that variabilities in velocity caused by successive shock waves are significant risk factors of freeway crashes. Chatterjee and Davis (2016) analyzed a rear-end crash mechanism caused by stopping shock waves on congested freeways. Furthermore, the well-known stability theory of general car-following models asserts that unstable traffic flow can propagate through a platoon and subsequently expose vehicles to higher crash risks (Leutzbach, 1988). From this perspective, an investigation of the impact of driving behavior on rear-end crash risk of the leading and following vehicles in a car-following situation is of great interest.

However, in a car-following situation, drivers differ and so are their driving styles. Thus, driving styles differ across drivers in traffic streams. This heterogeneity largely determines the traffic flow distribution and leads to shock waves (Kerner and Klenov, 2004). Hoogendoorn et al. (2007) further showed that the extent of heterogeneity influences the propagation of disturbance through the flows of vehicles that drive on the same lane, which implies that the level of heterogeneity of car-following behavior is substantial. This finding was verified by Ossen and Hoogendoorn (2011), who used a large sample of trajectory observations. Moreover, past studies reported that drivers with different characteristics have an important influence on traffic flow stability (Zhu and Dai, 2008; Tang et al., 2010; Yu et al., 2010; Wang et al., 2011; Taylor et al., 2015). Driving behavior heterogeneity should therefore be considered in real-life traffic characterization considering that heterogeneity can lead to rear-end crash risks, as proven by previous findings. Therefore, an approach based on a car-following model is presented in the current study for rear-end crash risk analysis on the basis of driving behavior heterogeneity. This approach is necessary in studying the sensitivity of driving behavior and the heterogeneity related to rear-end crash risks. A suitable approach for car-following modeling to investigate the impact of heterogeneity of car-following behavior on rear-end crash risk is also a topic worth exploring.

Driving behavior is largely affected by the risk perception of drivers in actual traffic. Lu et al. (2012) proposed a desired safety margin (DSM) model that can simulate the different drivers' physiological and psychological characteristics, such as the driver's response time, sensitivity coefficients for acceleration or deceleration, and DSM. Human performances can be quantified by the subjective risk perception of drivers in real-life traffic. Thus, we not only consider the driver-specific parameters in establishing a car-following model but also embody the subjective risk perception of drivers in a car-following situation. In the car-following process, the driving style is mainly reflected by subjective risk perception, acceleration and deceleration sensitivity, and response time. It is thus more realistic to analyze the impact of different driving styles on rear-end crash risk based on aforementioned driving behavior characteristics.

The remainder of this paper is organized as follows. The objective and contributions of this study are introduced in Section 2. In Section 3, the DSM model is elucidated and the heterogeneity is introduced. Section 4 presents an analysis of the general statistical properties of all driving behavior parameters by adopting the Next Generation Simulation (NGSIM) datasets. In Section 5, the performance of the DSM model is verified by using the vehicle trajectories of the NGSIM dataset. The qualitative and quantitative analytical results of the impact of heterogeneity on rear-end crash risk in the car-following process are presented in Section 6. The conclusion section in Section 7 summarizes the obtained results.

2. Objectives and contributions

The objective of this study is to investigate the impact of heterogeneity of driving behavior on rear-end crash risk, and answer three questions regarding the heterogeneity of driving behavior. (1) How do driving style heterogeneity and the proportions of the different driving styles affect rear-end crash risk? (2) How do the five driving behavior parameters impact rear-end crash risk? (3) How are rear-end crash and its probability related to different driving styles? The contributions of this study are two-fold. First, this study is a pioneering work to exploring the effect of five driving behavior parameters, including upper and lower limits of DSM, sensitivity coefficients of acceleration and deceleration, and response time, on rear-end crash probability. Second, two critical factors influencing shock waves and rear-end crashes are revealed, namely, driving behavior characteristics and proportion of different driving styles. Exploring the influence of driving behavior characteristics on rear-end crash probability is useful to reduce rear-end crash risk in the car following process.

3. DSM model description

The DSM model was proposed by (Lu et al., 2013) to explain car-following dynamics on the basis of drivers' physiological and

psychological characteristics. The DSM car-following model is expressed by

$$a_n(t+\tau) = \begin{cases} \alpha_1(SM_n(t) - SM_{nDH}),\ SM_n(t) > SM_{nDH} \\ \alpha_2(SM_n(t) - SM_{nDL}),\ SM_n(t) < SM_{nDL} \\ 0,\ else \end{cases} \tag{1}$$

and

$$SM_n(t) = 1 - \frac{v_n(t)\cdot\tau_2 + [v_n(t)]^2/2d_n(t)}{x_{n-1}(t) - x_n(t) - l_{n-1}} + \frac{[v_{n-1}(t)]^2/2d_{n-1}(t)}{x_{n-1}(t) - x_n(t) - l_{n-1}} \tag{2}$$

where $a_n(t)$ is the acceleration of the following car at time t; SM_{nDH} is the upper limit of the DSM in the car-following situation; SM_{nDL} is the lower limit of the DSM in the car-following situation; α_1 and α_2 are the sensitivity coefficients for acceleration and deceleration; $SM_n(t)$ is the perceived safety margin (PSM) for drivers; τ is the response time, including driver's response time (τ_1) and that of the brake system (τ_2); $v_n(t)$ and $v_{n-1}(t)$ are the velocity of the n th and $(n-1)$ th vehicle at time t, respectively; $\Delta x_n(t) = x_{n-1}(t) - x_n(t)$ represents the headway between the $(n-1)$ th and the n th vehicles; $d_n(t)$ and $d_{n-1}(t)$ are the deceleration of the $(n-1)$ th and the n th vehicle at time t, respectively; and l_{n-1} is the length of the preceding vehicle.

Eqs. (1) and (2) comprise the DSM car-following model. We argue that the DSM car-following model represents a framework for modeling car-following behavior. However, the DSM model is not a normative model. Different drivers exhibit different driving characteristics in a car-following situation. In the DSM model, those driving characteristics are reflected in the lower limit of the DSM, upper limit of the DSM, sensitivity coefficients for acceleration and deceleration, and driver's response time. The heterogeneity of car-following behavior is introduced into the DSM model as follows:

$$a_n(t+\tau_1^{n(i)}+\tau_2) = \begin{cases} \alpha_1^{n(i)}(SM^n(t) - SM_{nDH}^{n(i)}),\ SM_n(t) > SM_{nDH}^{n(i)} \\ \alpha_2^{n(i)}(SM^n(t) - SM_{nDL}^{n(i)}),\ SM_n(t) < SM_{nDL}^{n(i)} \\ 0,\ else \end{cases} \tag{3}$$

and

$$SM^n(t) = 1 - \frac{\tilde{v}_n(t)\cdot\tau_2 + [\tilde{v}_n(t)]^2/2d_n(t)}{\tilde{x}_{n-1}(t) - \tilde{x}_n(t) - l_{n-1}} + \frac{[\tilde{v}_{n-1}(t)]^2/2d_{n-1}(t)}{\tilde{x}_{n-1}(t) - \tilde{x}_n(t) - l_{n-1}} \tag{4}$$

where the superscript n denotes the n th vehicle in the platoon; the superscript i indicates that the driver of the n th vehicle belongs to the i th type of driving styles; and $SM^n(t)$ represents the PSM. The vehicle index n with i th type of driving styles, which consists of the sensitivity parameters ($\alpha_1^{n(i)}$; $\alpha_2^{n(i)}$), response time of driver ($\tau_1^{n(i)}$), and the limits of DSM ($SM_{nDL}^{n(i)}(t)$, $SM_{nDH}^{n(i)}(t)$), is important because these driving behavior parameters differ from one another across different types of drivers.

4. Driving behavior parameters in the car-following situation

The DSM model contains five parameters, namely, acceleration sensitivity to the difference between PSM and upper limit of DSM, deceleration sensitivity to the difference between PSM and lower limit of DSM, reaction time of a driver to the motion of a preceding vehicle, and upper and lower limits of the acceptable safety margin interval in the car-following process. Different driving behavior parameters can be determined by adjusting the values of these five driving behavior parameters in the DSM model. In analyzing the effect of the five driving behavior parameters, the vehicle trajectories in one of the NGSIM I-80 datasets are used. The five driving behavior parameters are assumed to be uniformly distributed over the following intervals: $\alpha_1, \alpha_2 \in [3, 30]$, $\tau \in [0.3, 2]$, and $SM_{nDL}, SM_{nDH} \in [0.5, 1]$. The first-order sensitivity indices of the five driving behavior parameters are calculated by variance-based sensitivity analysis. First-order sensitivity can characterize the contribution value of input variable to output variable, which is introduced as follows:

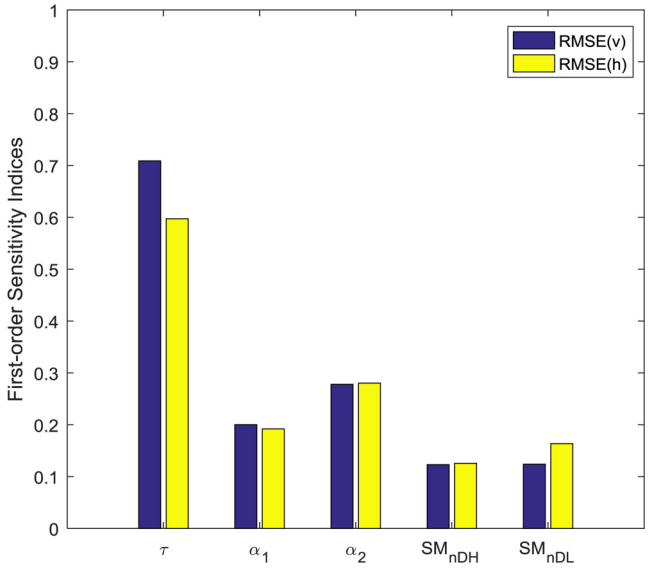

Fig. 1. First-order sensitivity indices based on RMSE(v) and RMSE(h) of the five driving behavior parameters.

$$S_i = \frac{V_{X_{\sim i}}(E_{\bar{X}_{\sim i}}(Y|\ X_i))}{V(Y)}, \tag{5}$$

where

$$V(Y) = V_{X_i}(E_{\bar{X}_{\sim i}}(Y|\ X_i)) + E_{X_i}(V_{\bar{X}_{\sim i}}(Y|\ X_i)). \tag{6}$$

In Eq. (6), X_i is the i th factor, $\bar{X}_{\sim i}$ denotes the vector of all factors except X_i, and Y is the output variable. The factor X_i includes the five driving behavior parameters, namely, acceleration and deceleration sensitivity coefficients, response time, and upper and lower limits of DSM. Y is either the root mean square error of velocity $RMSE(v)$ or the root mean square error of space headway $RMSE(h)$. $E(\cdot)$ and $D(\cdot)$ is the expectation and variance, respectively.

As shown in Fig. 1, the influences of the parameters can be thoroughly evaluated by using the first-order sensitivity index. This figure also shows that the deceleration sensitivity coefficient has a stronger influence on vehicle trajectory than the acceleration sensitivity coefficient. Furthermore, the lower limit of the DSM has a stronger influence on vehicle trajectory than the upper limit of the DSM, and the response time is the dominant influencing factor. It shows that the different behavior parameters clearly affect traffic flow patterns and cause shock waves, and this scenario likely increases rear-end crash risks. And it further imply that this five driving behavior parameters play key roles on avoidance of rear-end collision in the car-following process. Therefore, the driving behavior parameters should be calibrated, and the influences of these parametric variations on rear-end crash risk are investigated.

Here, we use 50 car-following cases, which are taken from the vehicle trajectory dataset of the Federal Highway Administration's NGSIM program, to calibrate the driving behavior parameters based on the DSM model.

4.1. Sensitivity parameters α_1 and α_2

The sensitivity parameters of the 50 car-following cases are calibrated by using the genetic algorithm (GA). The following results are obtained: the mean of α_1 is approximately 8.98 m/s^2, the standard deviation of α_1 is approximately 5.522 m/s^2, the mean of α_2 is approximately 15.20 m/s^2, and the standard deviation of α_2 is 8.159 m/s^2.

In the DSM model, the parameters α_1 and α_2 describe the acceleration and deceleration preferences. If a driver displays preference for sudden acceleration or deceleration, then α_1 or α_2 may be increased.

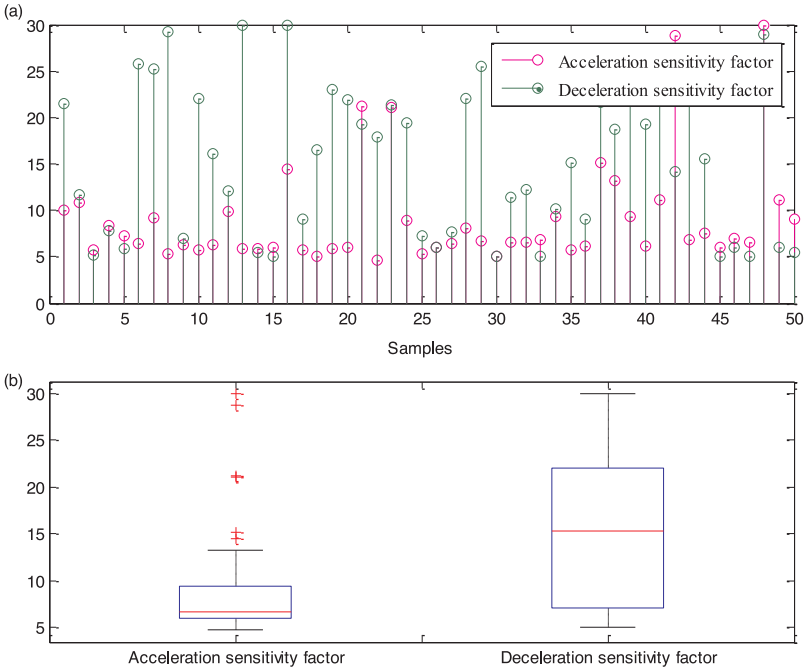

Fig. 2. Calibrated sample values and box plots of the α_1 and α_2.

Fig. 2(a) shows that different drivers have different sensitivity coefficients for acceleration and deceleration. Then, as shown in Fig. 2(b), the standard deviations of α_1 and α_2 are very high across different drivers. The results show that the drivers exhibit heterogeneity in terms of sensitivity to acceleration and deceleration.

4.2. Response time τ

In the DSM model, the response time includes the driver's reaction time (τ_1) and that of the brake system (τ_2). In this study, we mainly investigate the car-following response time of passenger car driver. The calibration results reveal that the response time ranges between 0.3 s and 2 s with a mean and a standard deviation of 0.73 s and 0.378 s, respectively. Sokolovskij (2010) found that "the values of the time of deceleration increase of most of the Japanese and Western vehicles have not exceeded 0.2 s and remained within the limits of 0.1–0.2 s." In emergency situations, the driver may quickly and strongly step on the brakes. Thus, we set τ_2 as 0.15 s in this study.

According to the statistical investigation of driving behavior (Ge et al., 2010), the range of a driver's reaction time is $\tau \in [0.3, 1.2]$. Fig. 3(a) confirms that the descriptive statistics of response time is reasonable, and the reaction time differs across drivers in a car-following situation. Fig. 3(b) shows that a certain difference exists among different drivers in terms of reaction time. The mean of driver's reaction time τ_1 is 0.58 s with a standard deviation of 0.378 s. These results imply that the drivers exhibit physiological heterogeneity in terms of car-following process.

4.3. Limit of the DSM parameters SM_{nDL} and SM_{nDH}

The interval $[SM_{nDL}, SM_{nDH}]$, an indicator of driving behavior when adjusting velocity, reflects a driver's psychological characteristics in the car-following process. Fig. 4(a) shows that different drivers exhibit certain differences in SM_{nDL} and SM_{nDH}. The corresponding mean values of SM_{nDL} and SM_{nDH} are 0.76 and 0.95, and their standard deviations are 0.125 and 0.045, respectively. Fig. 4(b) shows that SM_{nDL} and SM_{nDH} vary across different samples because different drivers have different risk perception levels in a car-following situation.

A large acceptable safety margin interval $[SM_{nDL}, SM_{nDH}]$ indicates that the driver does not prefer frequent adjustment in velocity. Conversely, a small acceptable safety margin interval $[SM_{nDL}, SM_{nDH}]$ indicates that the driver prefers frequent adjustment in velocity. Therefore, in the DSM model, the changes in the upper and lower limits of the acceptable safety margin interval have an important influence on a driver's acceleration and deceleration decision in a car-following situation. Overall, the results show that the drivers exhibit psychological heterogeneity in terms of car-following process.

4.4. Distribution and modeling of driving behavior parameters

To obtain the distribution function of the five driving behavior parameters and to model the parameters, we initially investigate whether a strong correlation exists between the upper and lower limits of DSM, response time, and acceleration and deceleration sensitivity coefficient in the aforementioned 50 cases.

The correlation coefficients of the five driving behavior parameters are shown in Table 1. No correlation exists; thus, all parameters are independent of one another. Accordingly, we estimate the general distribution of each driving behavior parameter. Kolmogorov–Smirnov (K–S) test is applied to the 50 cases. Five driving behavior parameters of the DSM model tend to follow the Johnson S_b distribution instead of other common distributions, such as uniform, normal, and Weibull distributions (Fig. 5). Given a confidence coefficient of 0.05, the P-values of the K–S statistics of the five driving behavior parameters are more than 0.05, as shown in Table 2. Therefore, the general distributions of the five driving behavior parameters obey the Johnson S_b distribution (γ, δ, λ, ξ), and their probability density function $f_{SB}(x)$ is given by

$$f_{SB}(x) = \frac{\delta}{\sqrt{2\pi}} \frac{\lambda}{(x-\xi)(\lambda+\xi-x)} \times \exp\left\{-\frac{1}{2}\left[\gamma + \delta \ln\left(\frac{x-\xi}{\lambda+\xi-x}\right)\right]^2\right\}, x \in [\xi, \xi+\lambda], \quad (7)$$

where λ is the scale parameter, γ and δ are the shape parameters, ξ is the positional parameter.

The different driving behavior parameters reflect different driving styles. Thus, we divide the drivers into different driving styles according to their driving behavior parameters in the car-following

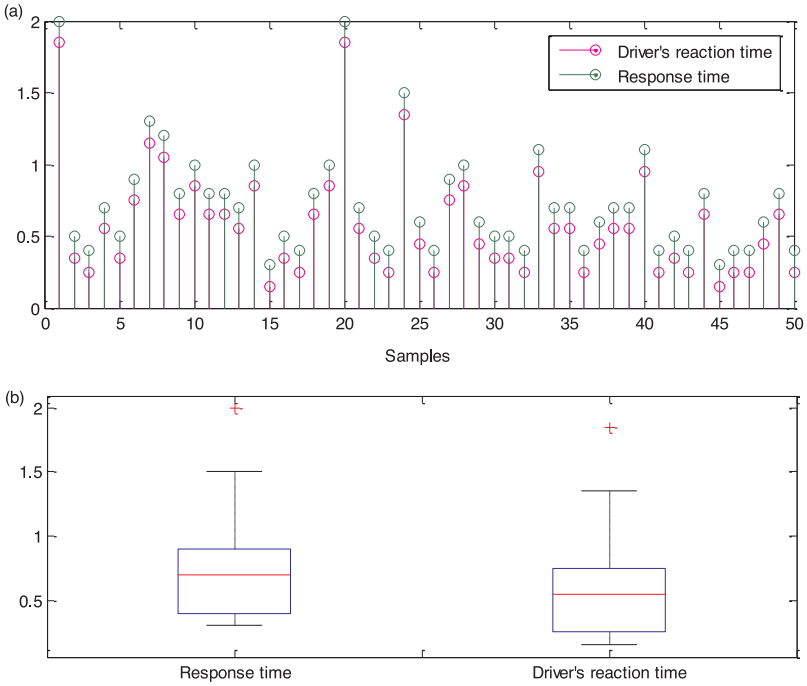

Fig. 3. Calibrated sample values and box plots of the τ and τ_1.

process. The classifications of the driving styles on the basis of the different driving behavior parameters are shown in Fig. 5(b). With regard to the sensitivity coefficients, the driving styles are classified as sensitive, normal, or insensitive. With regard to response time, the driving styles are classified as responsive, normal, or unresponsive. With regard to DSM, the driving styles are classified as risk-averse, normal, or risk-prone driving. We assume that each driving behavior parameter is roughly divided into three types, namely, type 1, normal, and type 2. Types 1 and 2 represent the corresponding driving behavior parameters. To avoid loss of generality, we assume that drivers who belong to type 1 and type 2 each account for 15%, whereas those

Table 1
The correlation coefficients of five driving behavior parameters.

Parameter	α_1	α_2	SM_{nDH}	SM_{nDL}	τ
α_1	1				
α_2	0.297	1			
SM_{nDH}	0.121	0.075	1		
SM_{nDL}	0.005	0.276	0.196	1	
τ	−0.115	0.352	0.192	0.211	1

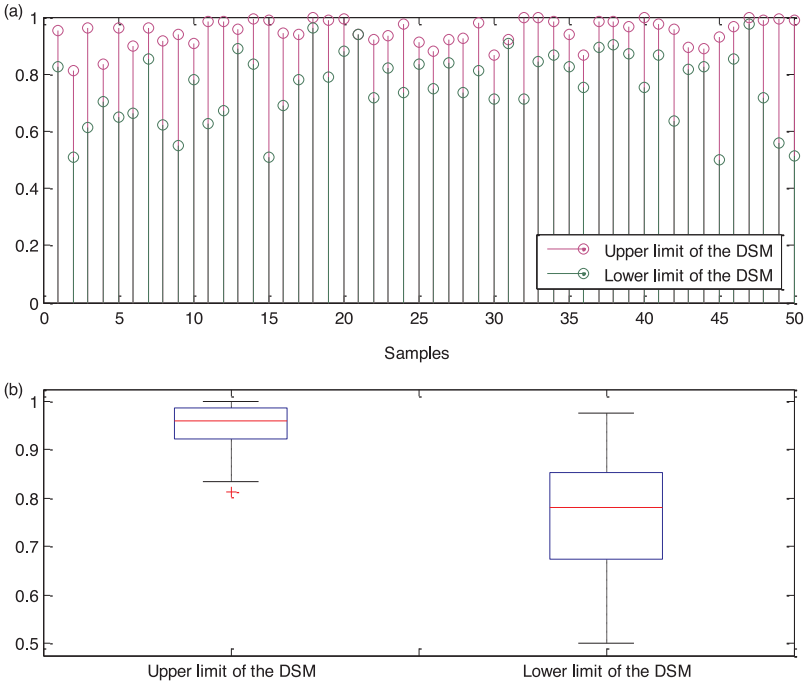

Fig. 4. Calibrated sample values and box plots of SM_{nDL} and SM_{nDH}.

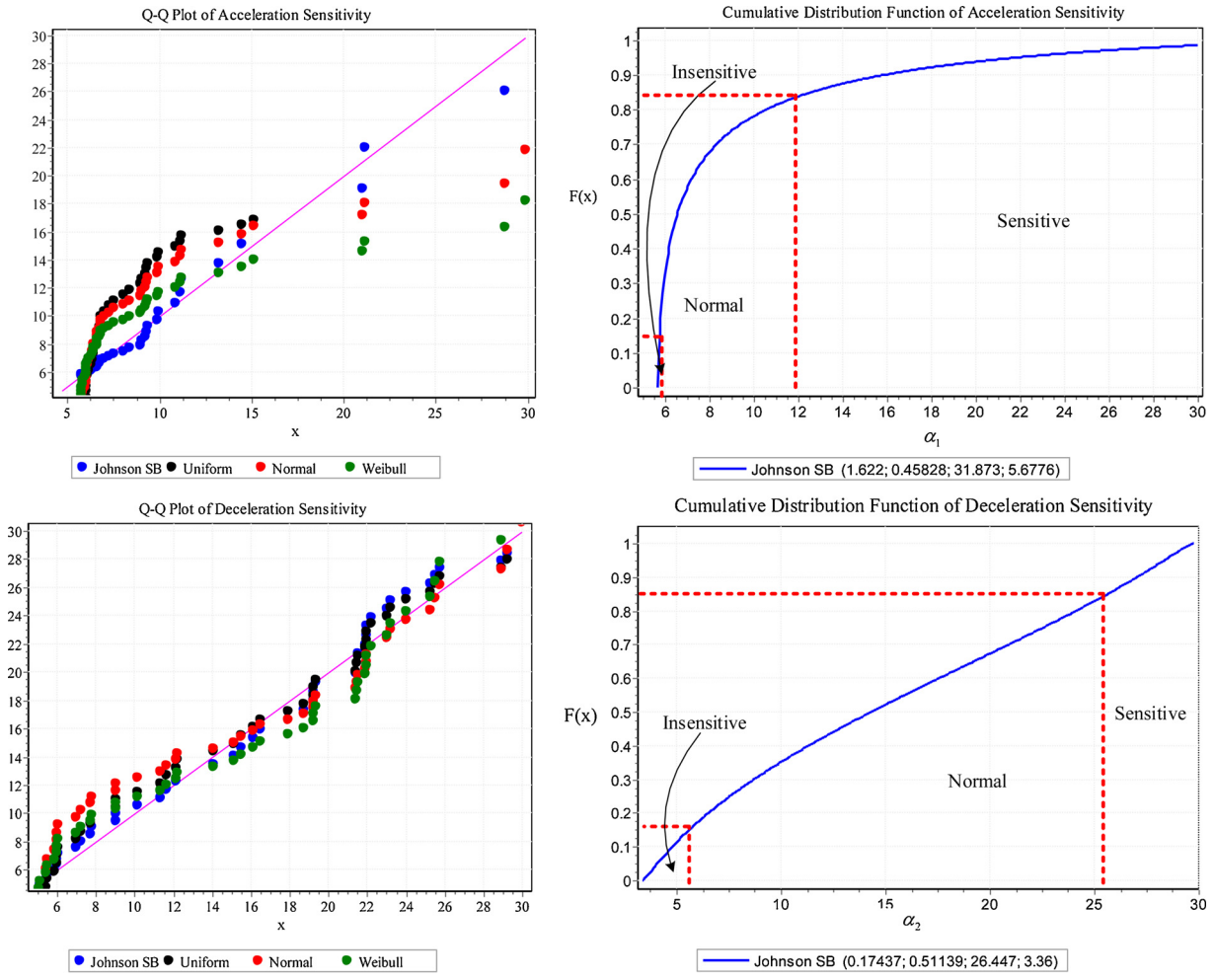

Fig. 5. Q-Q plots and Johnson SB distribution function of five driving behavior parameters.

drivers belonging to the normal type constitute 70%.

Different driving styles reflect the heterogeneity of the drivers. According to (Ossen and Hoogendoorn, 2011), heterogeneity has two types, namely, "driving style heterogeneity" and "heterogeneity within a driving style." Driving styles have different driving behavior parameters, which indicates that driving style heterogeneity exists ubiquitously and plays a key role in characterizing car-following behavior in real-life traffic situations. The characteristics of drivers are jointly determined by the five driving behavior parameters. In consideration of the driving style heterogeneity and individual differences of drivers with the same driving style, the five driving behavior parameters of the DSM model can be expressed as follows:

$$SM_{nDH}^{n(i)} = \overline{SM_{nDH}^{n(i)}} \pm \varepsilon \cdot \sigma^{SM_{nDH}^{n(i)}},\ F_{SM_{nDH}}^{-1}(\theta_{SM_{nDH}}^{i}) \le SM_{nDH}^{n(i)} \le F_{SM_{nDH}}^{-1}(\hat{\theta}_{SM_{nDH}}^{i}), \tag{8-1}$$

$$SM_{nDL}^{n(i)} = \overline{SM_{nDL}^{n(i)}} \pm \varepsilon \cdot \sigma^{SM_{nDL}^{n(i)}(t)},\ F_{SMlnDL}^{-1}(\theta_{SM_{nDL}}^{i}) \le SM_{nDL}^{n(i)} \le F_{SM_{nDL}}^{-1}(\hat{\theta}_{SM_{nDL}}^{i}), \tag{8-2}$$

$$\alpha_2^{n(i)} = \overline{\alpha_2^{n(i)}} \pm \varepsilon \cdot \sigma^{\alpha_2^{n(i)}},\ F_{\alpha_2}^{-1}(\theta_{\alpha_2}^{i}) \le \alpha_2^{n(i)} \le F_{\alpha_2}^{-1}(\hat{\theta}_{\alpha_2}^{i}), \tag{8-3}$$

$$\alpha_1^{n(i)} = \overline{\alpha_1^{n(i)}} \pm \varepsilon \cdot \sigma^{\alpha_1^{n(i)}},\ F_{\alpha_1}^{-1}(\theta_{\alpha_1}^{i}) \le \alpha_1^{n(i)} \le F_{\alpha_1}^{-1}(\hat{\theta}_{\alpha_1}^{i}), \tag{8-4}$$

$$\tau^{n(i)} = \overline{\tau^{n(i)}} \pm \varepsilon \cdot \sigma^{\tau^{n(i)}},\ F_{\tau}^{-1}(\theta_{\tau}^{i}) \le \tau^{n(i)} \le F_{\tau}^{-1}(\hat{\theta}_{\tau}^{i}), \tag{8-5}$$

where the superscript $-$ denotes the mean of each parameter; the superscript i denotes the type of driving styles; σ is the standard deviation of each parameter; θ^i and $\hat{\theta}^i$ are the lower and upper limits of the cumulative probability for the corresponding driving style i, respectively; and $F^{-1}(\cdot)$ is the cumulative probability function. In Eq. (8), ε obeys the standard normal distribution, that is, $\varepsilon \sim N(0, 1)$.

5. Verification of the DSM model

To investigate the impact of the heterogeneity of car-following behavior on rear-end crash risk by DSM modeling, we initially need to verify performance of the DSM model in simulating the entire car-following process. The analysis uses the vehicle trajectories of one of the "Lankershim" NGSIM datasets. This dataset was gathered from 8:30 a.m. to 8:45 a.m. The entire car-following model includes three traffic situations: start process, stop process, and platoon process.

We initially select three vehicles to investigate the vehicle trajectories in the start and stop processes in an intersection. The performance of the DSM model is also verified by comparing the measured values with the estimated vehicle trajectories in these two car-following processes. Then, we calibrate the driving behavior parameters of the DSM model by using GA owing to the driving style heterogeneity of the drivers.

During the simulations, the positions and velocities of the vehicles are updated at time step $\Delta t = 0.1s$ as follows:

$$v_n(t + \Delta t) = v_n(t) + \Delta t \cdot \dot{v}_n(t) \tag{9}$$

$$x_n(t + \Delta t) = x_n(t) + \Delta t \cdot \dot{x}_n(t) + \frac{1}{2}\ddot{x}_n(t) \cdot (\Delta t)^2 \tag{10}$$

where the dot denotes differentiation with respect to time.

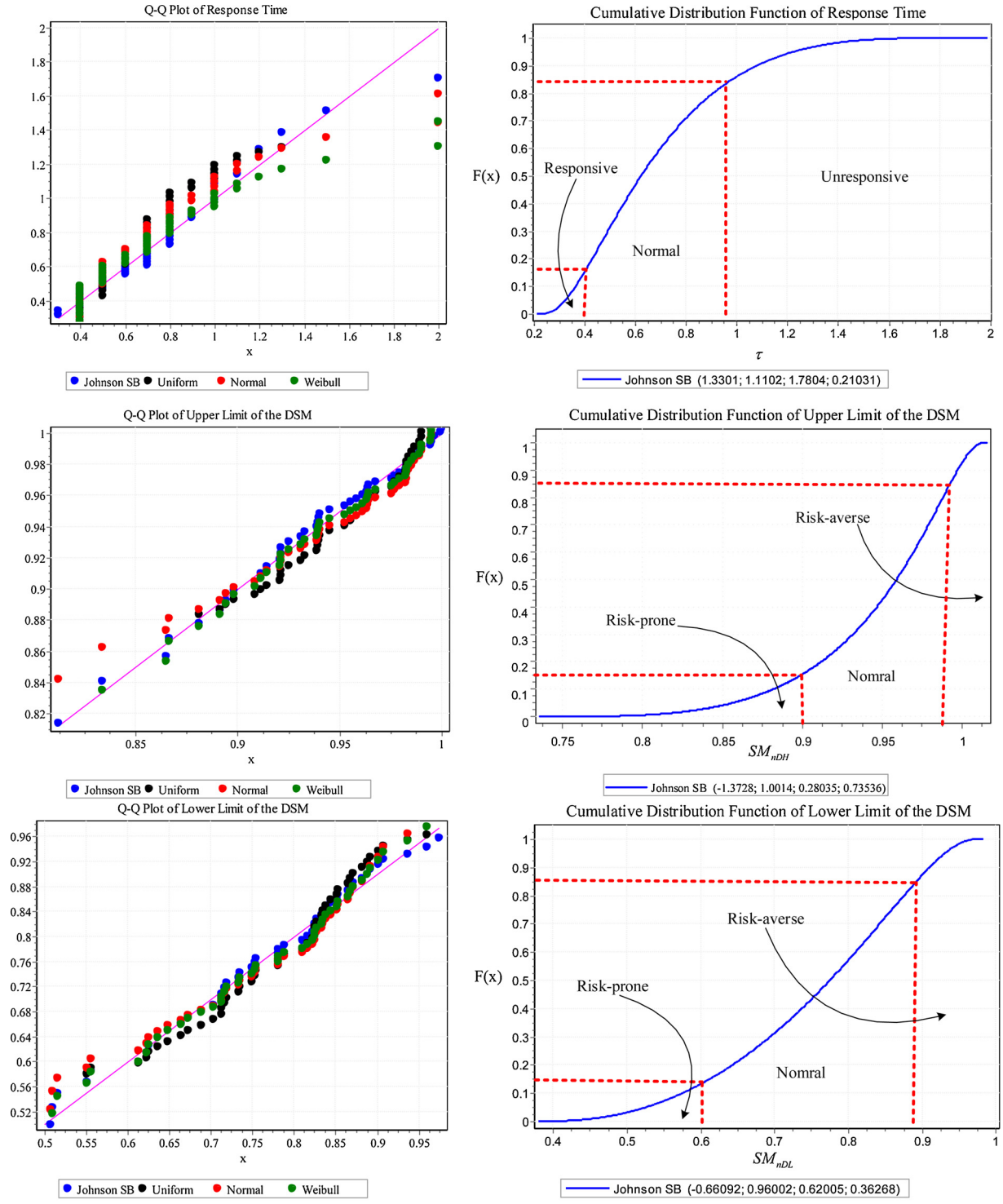

(a) Q-Q plots of different distribution functions (b) Johnson SB distribution function

Fig. 5. (*continued*)

Table 2
Results of K–S test for five driving behavior parameters.

Driving behavior parameter	Density distribution	P-value	$\alpha = 0.05$ (Are reject?)
α_1	Johnson SB	0.91	No
α_2		0.52	No
SM_{nDL}		0.93	No
SM_{nDH}		0.99	No
τ		0.36	No

5.1. Scenario 1. Start process

Initially, the traffic signal is red, and three vehicles are waiting behind the signal with nearly the same gap. The vehicles start to run at time $t = 0$ as the signal turns green. Subsequently, the leading vehicle starts to accelerate until it reaches an approximate fixed velocity of $v^* = 10$ m/s. Subsequently, we select a case to verify the performance of our proposed DSM model in the start process.

In this scenario, the velocity profiles are depicted in Fig. 6, in which

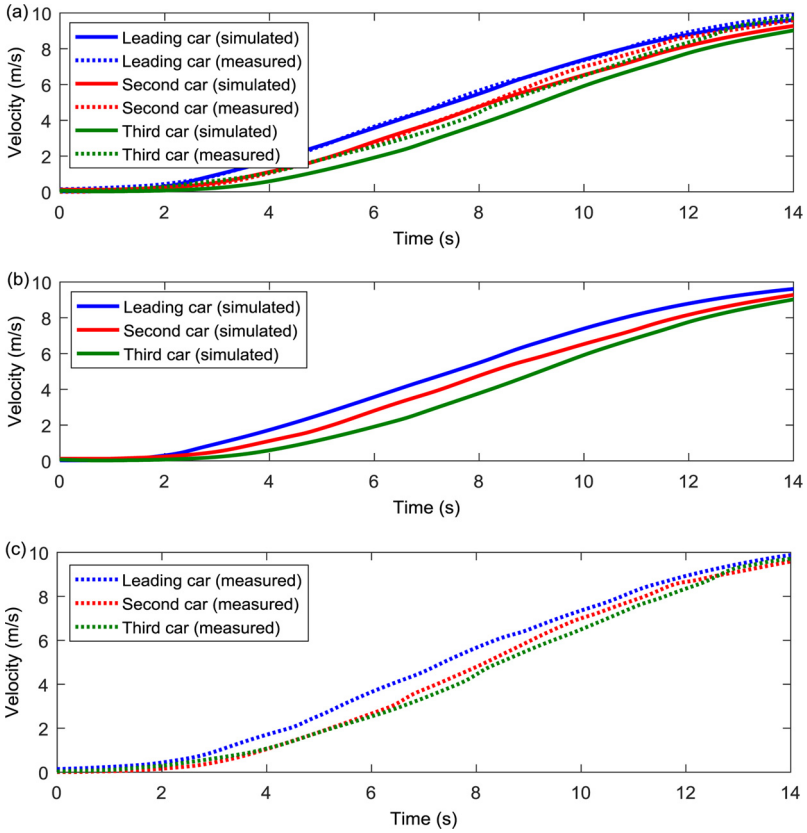

Fig. 6. Simulated and measured motions of vehicles 1–3 starting at a green traffic signal. Each curve shows the velocity of each vehicle (For interpretation of the references to colour in this figure legend, the reader is referred to the web version of this article).

Fig. 6(c) shows the motions of vehicles 1 (leading car), 2 (second car), and 3 (third car) starting from when the signal turned green. The motions are the measured values of the vehicle trajectories. Fig. 6(b) shows the DSM-based simulated motions of vehicles 1–3. Fig. 6(b) indicates that the vehicles can maintain the consensus state and finish the acceleration phase. Fig. 6(a) shows that the results of the DSM model resemble the measured data. Therefore, our proposed DSM model can effectively simulate the start process.

5.2. Scenario 2. Stop process

We also select a case to verify the performance of the DSM model in the stop process. Initially, the traffic signal is green, and the three vehicles are running on a single lane at nearly the same velocities and gaps. At time $t = 0$, the signal changes to red and vehicles 2 and 3 following the leading vehicle decelerate until all the vehicles reach a full stop.

The velocity profiles of the traffic stream stopping at a read signal are shown in Fig. 7. Although Fig. 7(a) shows certain errors between the results of the DSM model and the measured data, the vehicles can still maintain the consensus state and finish the deceleration phase according to the proposed DSM model, as shown in Fig. 7(b). The results of the DSM model resemble the measured data. Therefore, our proposed DSM model can effectively simulate the stop process.

5.3. Scenario 3. Platoon process

In the platoon process, the leading car, which exhibits a small speed perturbation, may cause a backward-propagating perturbation in the platoon. This backward wave will enlarge or shrink because of the random nature of driving. According to Castillo (2001), three types of propagation of perturbation occur randomly in car-following situations, namely, stable, decayed, and enhanced propagation, which are believed to be induced by the heterogeneity of driving behavior. However, normative models cannot simulate the randomness properties of dynamic traffic. To verify the DSM model with consideration of heterogeneity, we perform numerical simulation experiments.

All the vehicles (vehicle number $N = 50$) move on a single lane under an open boundary with a vehicle spacing of $L = 40$, as shown in Fig. 8. Furthermore, the initial positions and velocities of all the vehicles are supposed to be defined as

$$x_n(0) = L{\cdot}N,\ v_n(0) = 20,\ \dot{v}_n(0) = 0,\ n = 2,\ \cdots,N. \tag{11}$$

We assume that the leading vehicle moves at an initial velocity of 20 m/s. In the course of time, it decelerates to a velocity of 8 m/s at a deceleration rate of $-4\ \mathrm{m/s^2}$ and then accelerates to an initial velocity at an acceleration rate of $2\ \mathrm{m/s^2}$ after 6 s. Based on our proposed model expressed in Eqs. (3) and (4), the model parameters used in the simulations are $\tau_2 = 0.15$ s, $d_n(t) = d_{n\text{-}1}(t) = 7.35\ \mathrm{m/s^2}$, $l_n = 4.3$ m, and $n = 1,2,3,\cdots,N$. The five driving behavior parameters of the DSM model each generate 50 random numbers based on Eq. (8).

The numerical results of the iterative simulations of the DSM model are shown in Fig. 9. The findings indicate that three space–time plots of the traffic flow diagram may occur in dense traffic. Furthermore, Fig. 9 shows a backward propagating traffic wave with the introduction of an external disturbance into the uniform traffic flow. Fig. 9(a) shows that the perturbation maintains a steady state and spreads backward. The propagation of perturbation is gradually enhanced with an increase in the number of vehicles, as shown in Fig. 9(b). In Fig. 9(c), the propagation of the perturbation gradually dissipates. These results imply that the flow state of real-life traffic can be simulated by the DSM model, which performs well in simulating the heterogeneity of driving styles. Three types of perturbation propagation may be presented in dense traffic, and this finding is consistent with the relevant empirical

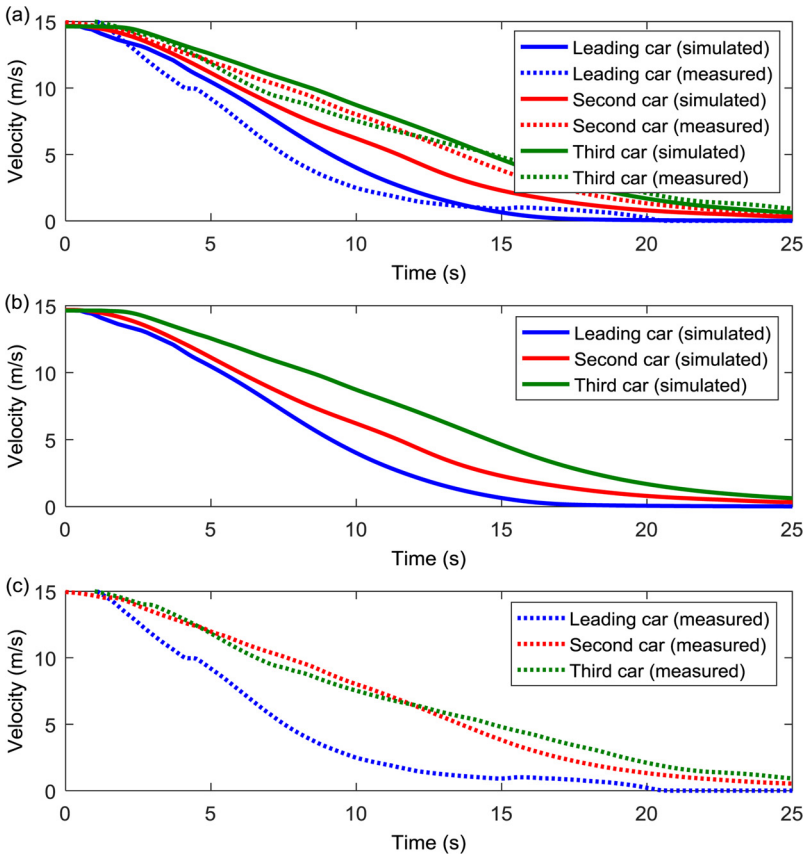

Fig. 7. Simulated and measured motions of vehicles 1–3 stopping at a red traffic signal. Each curve shows the velocity of each vehicle (For interpretation of the references to colour in this figure legend, the reader is referred to the web version of this article).

observations in previous studies ((Castillo, 2001) (Forbes and Simpson, 1968)). Thus, the DSM model can effectively describe the driving behavior in car-following situations. The results also indicate that heterogeneity can affect traffic flow patterns, and the shock wave it causes can in turn increase rear-end crash risk in the car-following process. In summary, the influence of heterogeneity on rear-end crash risk can be analyzed by using the DSM model.

6. Qualitative and quantitative analysis of rear-end crash risk

6.1. Qualitative analysis of the impact of the proportions of the different driving styles on rear-end crash risk

The impact of driving style heterogeneity on rear-end crash risk is numerically illustrated by investigating the time evolution of velocity. A small perturbation is also introduced. The following initial conditions are selected:

$$\begin{cases} x_1(0) = L{\cdot}N,\ v_1(0) = 20,\ \dot{v}_1(0) = 0, \\ \dot{v}_1(t) = \varepsilon_1(\hat{t}),\ t \geq \hat{t}, \\ x_n(0) = L{\cdot}(N-n+1),\ v_{n-1}(0) = 20,\ \dot{v}_{n-1}(0) = 0,\ n = 2,\cdots,N-1, \end{cases} \tag{12}$$

where the vehicle spacing L in the initial state is 30 m; the vehicle number N is 50; $x_n(0)$ represents the initial position of the n th vehicle in the system at time $t = 0$; $v_n(0)$ represents the initial velocity of the n th vehicle in the system at time $t = 0$; $\dot{v}_n(0)$ represents the initial acceleration of the n th vehicle in the system at time $t = 0$; and $\varepsilon_1(\hat{t})$, which follows the uniform random distribution $U(-1, 1)$ with amplitude 5×10^{-3}, is a small acceleration fluctuation of the first vehicle in the system after time delay $\hat{t}$.

With Eq. (8), we randomly generate 50 drivers as a basic case. Thus, the platoon basically conforms to the normal car-following situation. Subsequently, we consider several cases in the comparative study, and performed numerous numerical simulation tests to investigate the impact of the proportions of the different driving styles on rear-end crash risk.

The following cases are considered: case 1: increase in other driving styles except the normal driving style by 10%; case 2: increase in other driving styles by 20%; case 3: increase in other driving styles by 30%; and case 4: increase in other driving styles by 40%.

In all cases, the total number of drivers is 50 in the platoon. All drivers in the platoon are arbitrary and can perform randomness. In Fig. 10(a)–(e), the spatial–temporal patterns of the shock wave are enhanced from 0 s to 1000s under the proportions of the different driving styles. By contrast, in Fig. 10(a1)–(e1), the spatial–temporal patterns of the shock wave weakened from 0 s to 1000s under the proportions of the different driving styles. Fig. 10(a) shows that the disturbance propagation of the leading car results in a large fluctuation of the vehicles with the increase in the number of vehicles in the rear part of platoon. However, Fig. 10(a1) shows that the disturbance propagation of the leading car does not cause large fluctuations for vehicles in the rear part of platoon. The different degrees of self-stability of each driver can elicit such results through the randomly oriented drivers in the platoon. The results are in accordance with the relevant empirical observations results of previous studies Castillo (2001); Forbes and

Fig. 8. A platoon of N vehicles moving on a single lane.

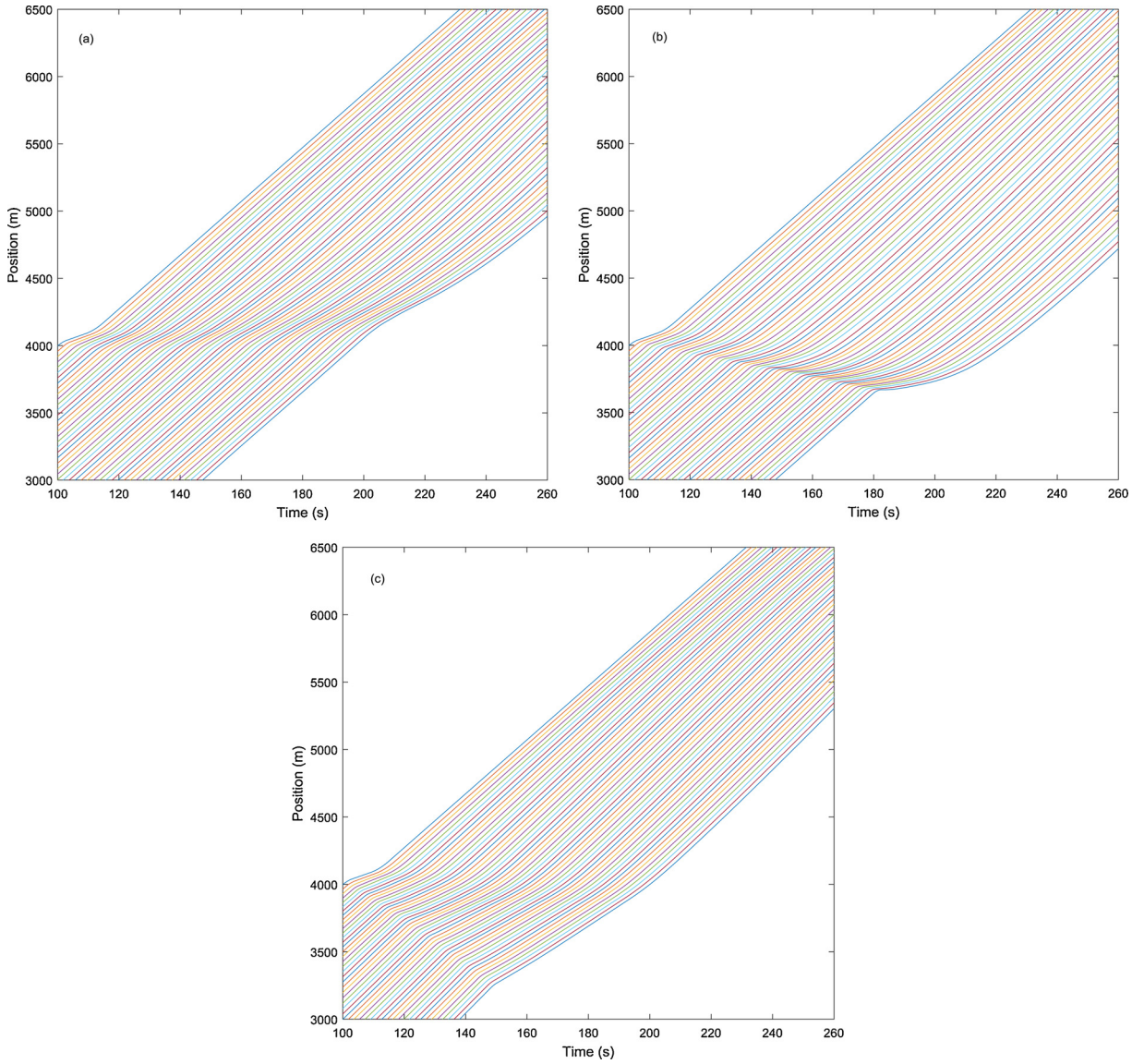

Fig. 9. DSM-based time–space diagrams of: (a) stable propagation of perturbation, (b) enhanced propagation of perturbation, and (c) decayed propagation of perturbation. Each line corresponds to a vehicle trajectory.

Simpson (1968) as discussed in the previous section. With adjustments in the proportions of the different driving styles of the platoon, the traffic flow patterns also change in different degrees. In contrast to Fig. 10(a)–(b), (b)–(b1) shows that the shock wave is enhanced with a 10% increase in others driving styles. However, as shown in Fig. 10(c), the fluctuation of the vehicles in the rear part of the platoon gradually becomes smaller than that in Fig. 10(b) when the other driving styles are increased by 20%. As shown in Fig. 10(d), backward propagating shock waves appear, and rear-end crashes may occur when the other driving styles are increased by 30% in the platoon. Fig. 10(e) shows that the probability of rear-end crashes considerably increase when the other driving styles are increase by 40%. By contrast, in Fig. 10(d1) and (e1), rear-end crashes will not occur, instead a more stable traffic flow will ensue. However, the increases in driving styles are different between Fig. 10(d) and (d1) and between Fig. 10(e) and (e1). For instance, the types of driving styles in Fig. 10(e) are fewer than those in Fig. 10(e1). These results imply that the shock wave depends on two critical factors: the proportions of the different driving styles and the driving behavior characteristics. Therefore, the proportions of the different driving styles and different driving behavior characteristics induce the occurrence and dissipation of the shock wave and increase rear-end crash risk. Given that the model parameters reflect the driving behavior characteristics, approximately 3^5 driving styles may be present according to Fig. 5. In this study, we assume that those driving styles are divided into two major categories, namely, stable driving style and unstable driving style. In other words, if stable and unstable driving styles coexist, their proportions will have a key influence on rear-end crash risk, as evident in the comparison of Fig. 10(a) and (e).

6.2. Quantitative analysis of rear-end crash risk with risk indicators

In this subsection, we perform the same simulation numerous times to obtain the change in the mean of two risk indicators in two situations. The basic case represents the situation in which all drivers in the platoon fall into the driving styles from the Johnson S_b distribution function of the five driving behavior parameters based on Eq. (8). In case 1, the drivers in the platoon exhibit half of the normal driving behavior characteristics and half of the insensitive, responsive, and risk-averse driving styles. In case 2, the drivers in the platoon have many driving styles, that is, all driving behavior parameters possess wide ranges compared with those in other cases.

In the platoon, the initial conditions of the vehicles are shown in Eq.

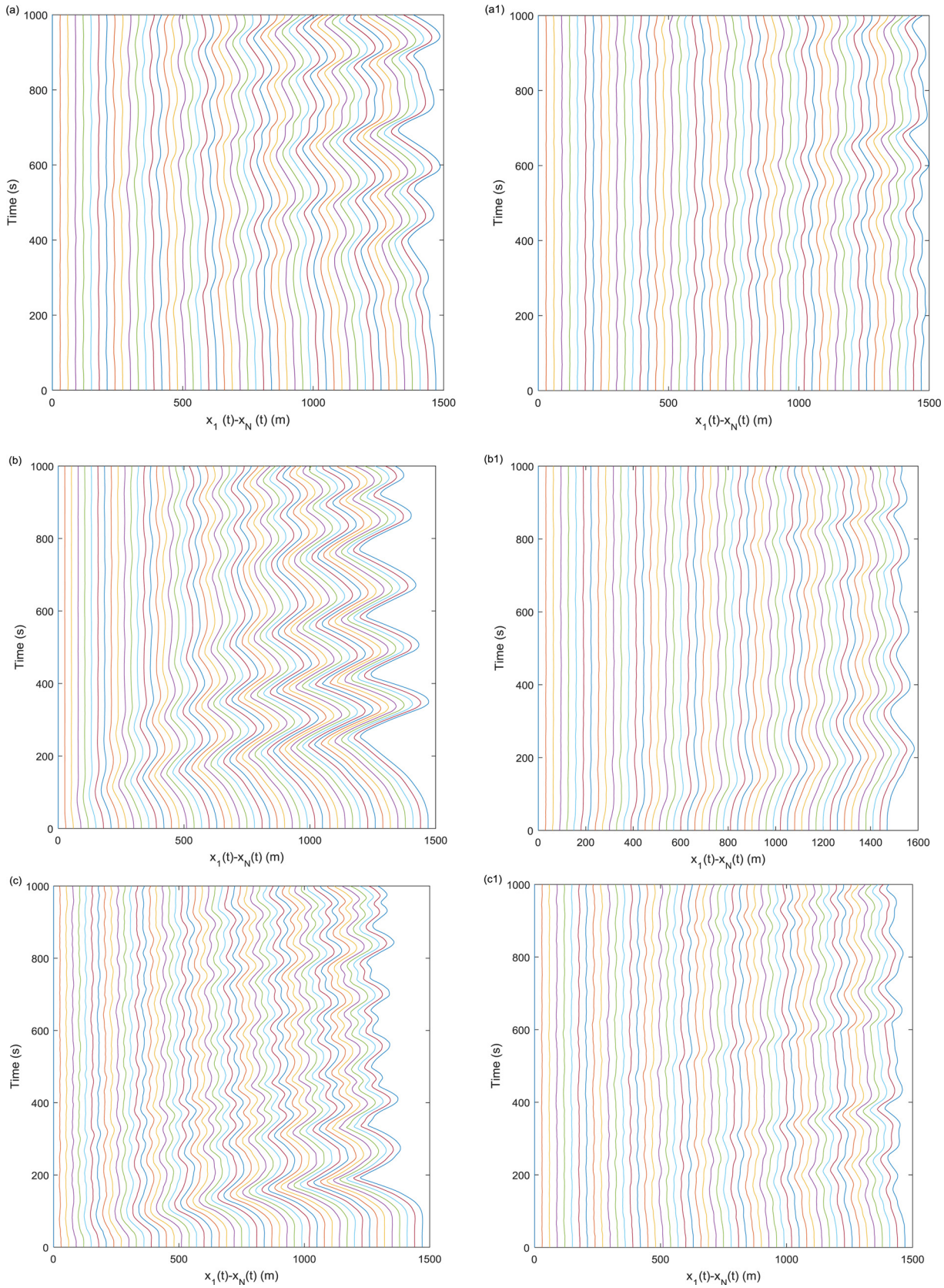

Fig. 10. Spatial–temporal patterns of the shock wave under different proportions of the different driving styles: (a)–(a1) basic case, (b)–(b1) case 1, (c)–(c1) case 2, (d)–(d1) case 3, and (e)–(e1) case 4.

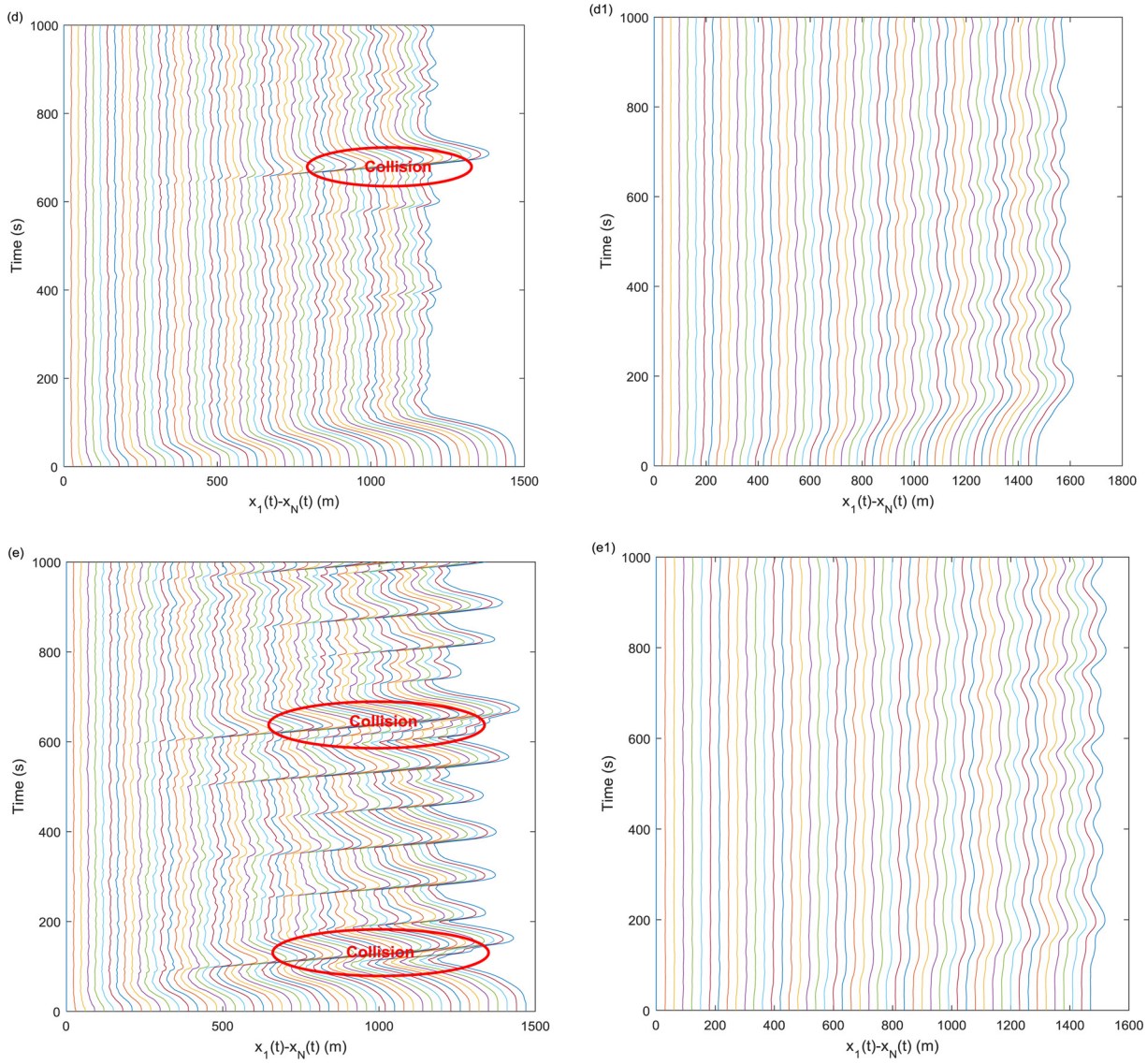

Fig. 10. (*continued*)

(11), where 20 vehicles are uniformly distributed on the straight road with a space headway of 40 m and a velocity of 15 m/s. In the car-following process, the leading vehicle brakes at $-1.5\,m/s^2$ for two short intervals (i.e., 200–203 s and 250–253 s) and then accelerates at $1.5\,m/s^2$ for two short intervals (i.e., 205–208 s and 255–258 s). These external disturbances are introduced to investigate the effect of heterogeneity on rear-end crash risk.

In the car-following process, time-to-collision (TTC) and time headway (TH) are typically used to describe risk. TTC is the time that remains until collision occurs when both continue on the same course. TH is the time difference between the consecutive arrival instances of two vehicles passing the measurement point on a lane. However, the effect of relative velocity is disregarded in the formulation of TH; thus, risk at a high relative velocity may be underestimated. Therefore, in this study, we select TTC as a risk indicator, which can be computed as follows:

$$TTC_n = \frac{\Delta x_n(t) - l_{n-1}}{v_n(t) - v_{n-1}(t)},\ \forall\ v_n(t) > v_{n-1}(t). \tag{13}$$

Furthermore, the safety margin (SM) can also be used as a risk indicator based on homeostatic risk perception in car-following situations. In the DSM model, the SM is simplified as follows:

$$SM_n = 1 - \frac{0.15 \cdot v_n(t) + [v_n(t)]^2/1.5g}{\Delta x_n(t) - l_{n-1}} + \frac{[v_{n-1}(t)]^2/1.5g}{\Delta x_n(t) - l_{n-1}}. \tag{14}$$

Here, we select vehicles 5, 15, and 20 as the target vehicles in our investigation of the difference between the two risk indicators in the given three cases. In the car-following process, the TTC of vehicles changes sharply; thus, a high or even an undefined TTC value may be obtained when the velocities of two successive vehicles in the platoon are nearly equal. To avoid this, 1/TTC is used to represent TTC in this study. Fig. 11 illustrates the 1/TTC and SM of vehicles 5, 15, and 20. As shown in Fig. 11(a), the 1/TTC values of the three vehicles tend to zero in case 2, but the fluctuation of 1/TTC increases in the basic case and case 1 when external disturbances are introduced into the platoon. For the homeostatic risk perception indicator SM, Fig. 11(b) shows that the SM values of the three vehicles all change in the range of 0.9–1 in case 2. However, the SMs of all the vehicles fluctuate within a wide range. Moreover, the SM value sometimes decreases to approximately 0.6 in the basic case and case 1. A comparison of the basic case and case 1 shows that the insensitive, responsive, and risk-averse driving styles can reduce rear-end crash risk; thus, these types of driving styles can be considered stable driving styles, which are conducive for producing a smooth shock wave. This result implies that increasing stable driving styles can reduce rear-end crash risk in the car-following process and

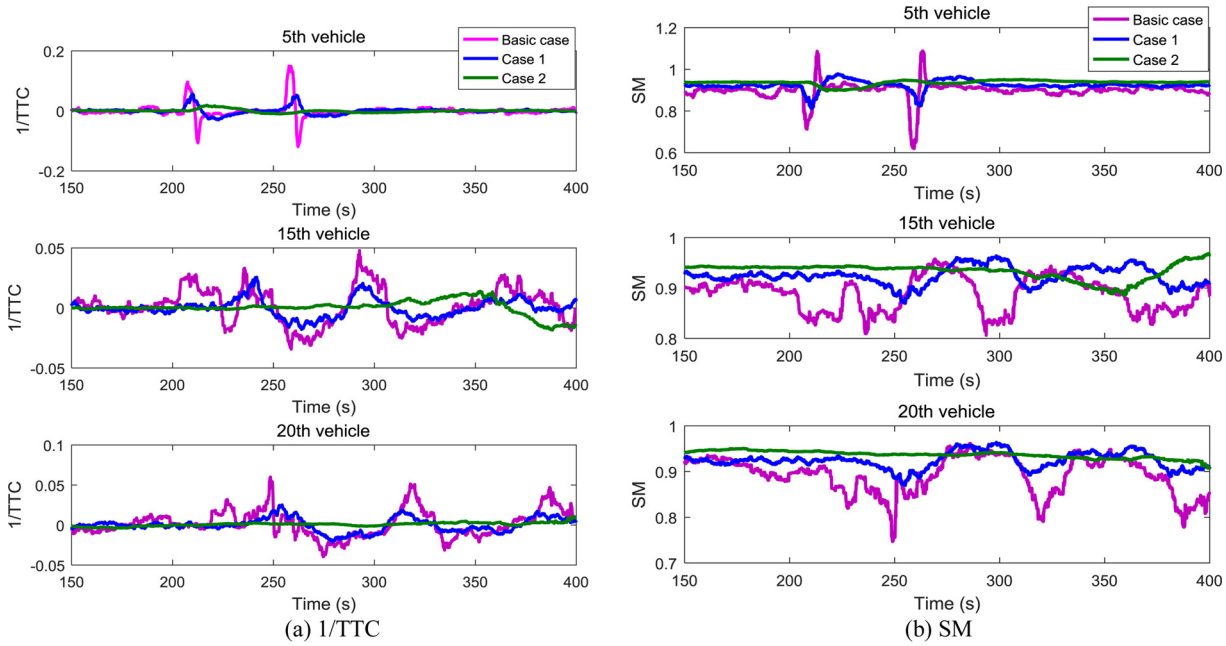

Fig. 11. 1/TTC and SM of vehicles 5, 15, and 20 under different driving styles.

may be a potential method to avoid rear-end crashes. Moreover, the rear-end crash risk in case 2 is lower than those in the other two cases. This result indicates that a wide extent of driving behavior heterogeneity can attenuate shock waves and agrees with the finding of Mason and Woods (1997). Therefore, the rear-end crash risk in case 2 is reduced compared with that in case 1. In summary, heterogeneity has an important impact on rear-end crash risk. The five driving behavior parameters used in this study can determine the driving styles, and exploring the effect of each on rear-end crash probability is useful for urban road traffic control and can provide an improved understanding of abnormal driving behavior characteristics to minimize rear-end crash risk.

6.3. Sensitivity analysis of the five driving behavior parameters based on a logistic regression model

As previously discussed, different driving styles may increase rear-end crash risk in the car-following process. Thus, the relationship between rear-end crash risk and the driving behavior parameters should be understood.

In this subsection, the sensitivity of each of the five driving behavior parameters to rear-end crash probability is analyzed. In the platoon, the vehicle spacing L in the initial state is 40 m, and the vehicle number N is 10. Furthermore, the initial positions and velocities of all vehicles are defined as follows:

$$x_n(0) = L{\cdot}N,\ v_n(0) = 15,\ \dot{v}_n(0) = 0,\ n = 2,\ \cdots, N.$$

As suggested by (Treiber et al., 2013), the leading vehicle brakes at $-1.5\ \mathrm{m/s^2}$ for a short interval (i.e., 200–202 s) and then accelerates at $1\ \mathrm{m/s^2}$ for a short interval (i.e., 204–207 s). We take this external disturbance as a traffic condition in the car-following process.

In accordance with the study of (Hair et al., 2013), a binary logistic regression is used in the current study because the dependent variable C (rear-end crash) can only have two values: $C = 1$ for rear-end crashes, and $C = 0$ for non-rear-end crashes. Accordingly, the logistic regression model can be expressed as

$$P(C = 1|\ X) = \frac{\exp(g(X))}{1 + \exp(g(X))}, \tag{15}$$

$$g(X) = \ln\left[\frac{P(X)}{1 - P(X)}\right] = \beta_0 + \beta_1 X_1 + \beta_2 X_2 + \cdots + \beta_n X_n, \tag{16}$$

where $P(C = 1|\ X)$ is the conditional probability of a rear-end crash, X_n are independent variables (driving behavior parameters), and β_n is a model coefficient that directly determines the odds ratio involved in the rear-end accident.

We select 10,000 samples in random combinations of the five driving behavior parameters by using Monte Carlo stochastic simulation method. The results of the logistic regression analysis of the model are summarized in Table 3. The value of χ^2 in the logistic equation is high (i.e., 37.236). The accuracy rate of classification in this study is defined as the ratio of the correctly estimated rear-end crashes (determined by logistic regression model) to the total number of crashes (for analysis). A cut-off value of 0.5 is used for computing the classification rate. The results indicate that the proposed model can predict rear-end crashes with a high degree of accuracy. The constant and coefficient estimates of the model are statistically significant. In Table 3, the response time τ, the lower limit of the DSM SM_{nDL}, and the upper limit of the DSM SM_{nDH} are the contributing factors that influence the rear-end crashes, whereas the acceleration sensitivity coefficient α_1 and the deceleration sensitivity coefficient α_2 do not show a strong contribution to the rear-end crashes. The signs of the coefficients of the independent variables for τ and α_1 are negative, indicating that the vehicles in the platoon are likely to be involved in rear-end crashes when the drivers are unresponsive and sensitive to acceleration. Furthermore, high upper and lower limits of the DSM (positive values for

Table 3
Results of the logistic regression analysis.

Parameters	β	S.E.	Wals	Sig.	Exp (β)
τ	2.569	0.079	1069.932	0.000	13.047
SM_{nDL}	−1.294	0.188	47.404	0.000	0.274
SM_{nDH}	−4.320	0.532	65.896	0.000	0.013
α_1	0.001	0.004	0.045	0.832	0.999
α_2	−0.002	0.003	0.648	0.421	1.002
Constant	1.537	0.530	8.414	0.004	4.651

S.E., Wals, Sig., and Exp(β) represent standard error, Wald statistic, significance, and odds ratio, respectively.
Model χ^2: 37.236; Nagellerke R^2: 0.139; Correct classification rate: 82.7%.

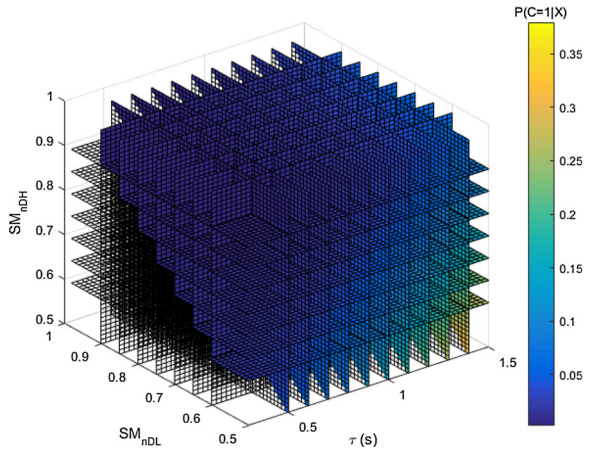

Fig. 12. Rear-end crash probability for three different driving behavior parameters (i.e., τ, SM_{nDL}, and SM_{nDH}).

SM_{nDL} and SM_{nDH}) and a high deceleration sensitivity coefficient (positive for α_2) can reduce rear-end crash risk. These results imply that the risk-averse and responsive drivers are propitious for the reduction of rear-end crash risk. Likewise, the drivers who are insensitive to acceleration and sensitive to deceleration can reduce rear-end crash risk. The probability model developed in this study with the estimated coefficients is expressed in Eq. (17).

$$P(C = 1|\ X) = \frac{1}{1 + \exp(-1.537 - 2.569\tau + 1.294SM_{nDL} + 4.320SM_{nDH} - 0.001\alpha_1 + 0.002\alpha_2)}. \quad (17)$$

To estimate the rear-end crash probability, Eq. (17) is used for the five driving behavior parameters. The estimation results can further verify the results of the logistic regression model-based qualitative analysis of rear-end crash risk in the car-following process. Fig. 12 shows the rear-end crash probability with variations in SM_{nDL}, SM_{nDH}, and τ. The effects of the acceleration and deceleration sensitivity coefficients effect on rear-end crash risk were disregarded because of their negligible impact. As shown in Fig. 12, the selection of DSMs and response time influences the rear-end crash probability, implying that different driving styles affect the rear-end crash risk in the car-following process. The results further show that the heterogeneity of car-following behavior impact rear-end crash risk, and the reasonable adjustment in driving styles can reduce the rear-end crash risk in the car-following process.

7. Conclusion

In the car-following process, drivers adjust their velocity on the basis of their subjective perception of risk. Risk perception is the key parameter of psychological behavior. The DSM model uses SM_{nDL} and SM_{nDH} to describe the psychological behavior, α_1 and α_2 to describe the operation behavior, and τ to denote the performance of the driver in terms of response time. Different drivers have different characteristics of acceleration or deceleration depending on risk perception. Therefore, the psychological behavior, operation behavior, and driver performance in terms of response time affect the level of car-following safety.

The impact of driving behavior heterogeneity is explored by calibrating the driving behavior parameters of the DSM model by using an NGSIM dataset. The driver types are clustered according to the driving behavior parameters. The drivers are classified as insensitive, normal, or sensitive on the basis of the acceleration and deceleration sensitivity coefficients. Drivers are classified as risk-averse, normal, or risk-prone on the basis of the DSM. Drivers are classified as unresponsive, normal, or responsive on the basis of the response time. On the basis of the car-following cases from the NGSIM dataset, we find that the general distributions of the five driving behavior parameters obey the Johnson S_b distribution. A global variance sensitivity analysis is performed, and the first-order sensitivity indices of the five driving behavior parameters show that these parameters affect traffic flow patterns. Moreover, numerical simulations are conducted to analyze the influence of heterogeneity on the rear-end crash risk in the car-following process. The drawn conclusions can be summarized as follows:

The two critical factors that affect shock waves are the driving behavior characteristics and the proportions of the different driving styles. Driving styles are divided into two categories, namely, stable and unstable. The stable driving style is conducive to the dissipation of shock waves and reduce rear-end crash risk. In addition, if the stable and unstable driving styles coexist, their proportions will have a key influence on the rear-end crash risk.

The quantitative risk indicators TTC and SM indicate that increasing the proportion of unstable driving styles cause a relatively high rear-end crash risk index, whereas increasing the proportion of stable driving styles can reduce the rear-end crash risk in the car-following process. Thus, the latter measure can potentially minimize rear-end crash risk. A wide extent of driving behavior heterogeneity can attenuate shock waves, thereby reducing rear-end crash risk. Thus, heterogeneity has an important impact on rear-end crash risk.

A decrease in the lower (or upper) limit of the DSM increasing the response time, decreasing the sensitivity coefficient for deceleration, or increasing the sensitivity coefficient for acceleration can increase rear-end crash risk. Risk-averse, responsive, and insensitive to acceleration (or sensitive to deceleration) driving styles with are conducive to the reduction of rear-end crash risk. Therefore, adjusting the proportions of unstable driving styles is a potential strategy for attenuating shock waves and reducing rear-end crash risk to a certain extent.

Overall, driving behavior heterogeneity has an important impact on rear-end crash risk. Furthermore, driving behavior determines driving styles. By adjusting the DSM, acceleration and deceleration sensitivity, and response time of a driver, relatively stable driving styles can be achieved to eliminate shock waves and reduce rear-end crash risk. Thus, exploring the effect of each driving behavior parameter on rear-end crash probability is useful for urban road traffic control which can provide an improved understanding of abnormal driving behavior characteristics to minimize rear-end crash risk

Acknowledgment

This work was supported by the National Natural Science Foundation of China (Grants U1664262, U1564212).

References

Anastasopoulos, P.C., Mannering, F.L., 2009. A note on modeling vehicle accident frequencies with random-parameters count models. Accid. Anal. Prev. 41 (1), 153.
Anastasopoulos, P., Mannering, F.L., Shankar, V.N., Haddock, J.E., 2012. A study of factors affecting highway accident rates using the random-parameters tobit model. Accid. Anal. Prev. 45 (2), 628.
Borowsky, A., Oron-Gilad, T., Meir, A., Parmet, Y., 2012. Drivers' perception of vulnerable road users: a hazard perception approach. Accid. Anal. Prev. 44 (1), 160.
Castillo, J.M.D., 2001. Propagation of perturbations in dense traffic flow: a model and its implications. Transp. Res. Part B Methodol. 35 (4), 367–389.
Chatterjee, I., Davis, G.A., 2016. Analysis of rear-end events on congested freeways by using video-recorded shock waves. Transp. Res. Rec. J. Transp. Res. Board 2583 (2583), 110–118.
Chin, H.C., Quddus, M.A., 2003. Applying the random effect negative binomial model to examine traffic accident occurrence at signalized intersections. Accid. Anal. Prev. 35 (2), 253–259.
Deublein, M., Schubert, M., Adey, B.T., Köhler, J., Faber, M.H., 2013. Prediction of road accidents: a bayesian hierarchical approach. Accid. Anal. Prev. 51 (4), 274.
Forbes, T.W., Simpson, M.E., 1968. Driver-and-vehicle response in freeway deceleration waves. Transp. Sci. 2 (1), 77–104.
Ge, R., Zhang, W., Wang, Z., 2010. Year. Research on the driver reaction time of safety distance model on highway based on fuzzy mathematics. Proceedings of the International Conference on Optoelectronics and Image Processing. pp. 293–296.
Geedipally, S.R., Lord, D., Dhavala, S.S., 2012. The negative binomial-lindley generalized

linear model: characteristics and application using crash data. Accid. Anal. Prev. 45 (1), 258.
Hair, J.F., Black, W.C., Babin, B.J., Anderson, R.E., Tatham, R.L., 2013. Multivariate data analysis. Technometrics 49 (1), 103–104.
Hoogendoorn, S.P., Ossen, S., Schreuder, M., 2007. Year. Properties of a microscopic heterogeneous multi-anticipative traffic flow model. Proceedings of the Transportation and Traffic Theory. Papers Selected for Presentation at ISTTT17.
Hourdos, J.N., 2005. Crash Prone Traffic Flow Dynamics : Identification and Real-Time Detection.
Huang, D.L., Yan, Y.S., Su, C., Xu, G.X., 2016. Prediction-based geographic routing over vanets. RevistaTecnica de la Facultad de Ingenieria Universidad del Zulia 39 (2), 157–164.
Jovanis, P.P., Chang, H.L., 1986. Modeling the relationship of accidents to miles traveled. Transportation Research Record, No. 1068, TRB. National Research Council, pp. 42–51.
Kerner, B.S., Klenov, S.L., 2004. Spatial–temporal patterns in heterogeneous traffic flow with a variety of driver behavioural characteristics and vehicle parameters. J. Phys. A Gen. Phys. 37 (37), 8753.
Kim, J.K., Wang, Y., Ulfarsson, G.F., 2007. Modeling the probability of freeway rear-end crash occurrence. J. Transp. Eng. 133 (1), 11–19.
Kim, S.K., Song, T.J., Rouphail, N.M., Aghdashi, S., Amaro, A., Gonçalves, G., 2016. Exploring the association of rear-end crash propensity and micro-scale driver behavior. Saf. Sci. 89, 45–54.
Lao, Y., Wu, Y.J., Corey, J., Wang, Y., 2011a. Modeling animal-vehicle collisions using diagonal inflated bivariate poisson regression. Accid. Anal. Prev. 43 (1), 220–227.
Lao, Y., Zhang, G., Wu, Y.J., Wang, Y., 2011b. Modeling animal-vehicle collisions considering animal-vehicle interactions. Accid. Anal. Prev. 43 (6), 1991–1998.
Lao, Y., Zhang, G., Wang, Y., Milton, J., 2014. Generalized nonlinear models for rear-end crash risk analysis. Accid. Anal. Prev. 62 (5), 9–16.
Lee, D.N., 1976. A theory of visual control of braking based on information about time-to-collision. Perception 5 (4), 437–459.
Leutzbach, D.I.W., 1988. Introduction to the Theory of Traffic Flow. Springer.
Li, Y., Zheng, Y., Wang, J., Kodaka, K., Li, K., 2017. Crash probability estimation via quantifying driver hazard perception. Accid. Anal. Prev.
Lord, D., Mannering, F., 2010. The statistical analysis of crash-frequency data: a review and assessment of methodological alternatives. Transp. Res. Part A Policy Pract. 44 (5), 291–305.
Lu, G., Cheng, B., Lin, Q., Wang, Y., 2012. Quantitative indicator of homeostatic risk perception in car following. Saf. Sci. 50 (9), 1898–1905.
Lu, G., Cheng, B., Wang, Y., Lin, Q., 2013. A car-following model based on quantified homeostatic risk perception. Math. Probl. Eng. (6), 165–185 (2013-11-18).
Mason, A.D., Woods, A.W., 1997. Car-following model of multispecies systems of road traffic. Phys. Rev. E Stat. Phys. Plasmas Fluids Relat. Interdiscip. Topics 55 (3), 2203–2214.
Meir, A., Borowsky, A., Oron-Gilad, T., 2014. Formation and evaluation of act and anticipate hazard perception training (aahpt) intervention for young novice drivers. Traff. Inj. Prev. 15 (2), 172.
Miaou, S.P., 1994. The relationship between truck accidents and geometric design of road sections: poisson versus negative binomial regressions. Accid. Anal. Prev. 26 (4), 471–482.
Miaou, S.P., Lum, H., 1993. Modeling vehicle accidents and highway geometric design relationships. Accid. Anal. Prev. 25 (6), 689–709.
Miaou, S.P., Hu, P.S., Wright, T., Rathi, A.K., Davis, S.C., 1992. Relationship Between Truck Accidents and Highway Geometric Design: a Poisson Regression Approach.
Ossen, S., Hoogendoorn, S.P., 2011. Heterogeneity in car-following behavior: theory and empirics. Transp. Res. Part C Emerg. Technol. 19 (2), 182–195.
Park, E.S., Lord, D., Professor, A., 2008. Multivariate poisson-lognormal models for jointly modeling crash frequency by severity. Transp. Res. Rec. J. Transp. Res. Board(2019).
Poch, M., Mannering, F., 1996. Negative binomial analysis of intersection-accident frequencies. J. Transp. Eng. 122 (2), 105–113.
Sokolovskij, E., 2010. Experimental investigation of the braking process of automobiles. Transport 20 (3), 91–95.
Tampere, C.M.J., Hoogendoorn, S.P., Arem, B.V., 2005. A Behavioural Approach to Instability, Stop and Go Waves, Wide Jams and Capacity Drop.
Tanaka, M., Ranjitkar, P., Nakatsuji, T., 2008. Asymptotic Stability and Vehicle Safety in Dynamic Car-following Platoon.
Tang, T.Q., Li, C.Y., Huang, H.J., 2010. A new car-following model with the consideration of the driver's forecast effect. Phys. Lett. A 374 (38), 3951–3956.
Taylor, J., Zhou, X., Rouphail, N.M., Porter, R.J., 2015. Method for investigating intradriver heterogeneity using vehicle trajectory data: a dynamic time warping approach. Transp. Res. Part B Methodol. 73, 59–80.
Treiber, M., Kesting, A., Thiemann, C., 2013. Traffic Flow Dynamics : Data. models and simulation Springer.
Wang, L., Zhang, H., Meng, H., Wang, X., 2011. The influence of individual driver characteristics on congestion formation. Int. J. Mod. Phys. C 22 (03), 305–318.
Weng, J., Meng, Q., 2014. Rear-end crash potential estimation in the work zone merging areas. J. Adv. Transp. 48 (3), 238–249.
Weng, J., Meng, Q., Yan, X., 2014. Analysis of work zone rear-end crash risk for different vehicle-following patterns. Accid. Anal. Prev. 72, 449–457.
Weng, J., Xue, S., Yang, Y., Yan, X., Qu, X., 2015. In-depth analysis of drivers' merging behavior and rear-end crash risks in work zone merging areas. Accid. Anal. Prev. 77, 51–61.
Weng, J., Zhu, J.Z., Yan, X., Liu, Z., 2016. Investigation of work zone crash casualty patterns using association rules. Accid. Anal. Prev. 92, 43–52.
Weng, J., Li, G., Yao, Y., 2017. Time-dependent drivers' merging behavior model in work zone merging areas. Transp. Res. Part C Emerg. Technol. 80, 409–422.
Weng, J., Du, G., Li, D., Yu, Y., 2018. Time-varying mixed logit model for vehicle merging behavior in work zone merging areas. Accid. Anal. Prev. 117, 328–339.
Wiedemann, R., Reiter, U., 1992. Microscopic traffic simulation, the simulation system mission, background and actual state. Project ICARUS (V1052) Final Report 2. pp. 1–53.
Wu, K.F., Thor, C.P., 2015. Method for the use of naturalistic driving study data to analyze rear-end crash sequences. Transp. Res. Rec. J. Transp. Res. Board 2518 (2518), 27–36.
Xiao, H., 2016. Continuous knn queries in dynamic road networks. RevistaTecnica de la Facultad de Ingenieria Universidad del Zulia 39 (4), 354–361.
Yu, L., Li, T., Shi, Z.K., 2010. Density waves in a traffic flow model with reaction-time delay. Phys. A Stat. Mech. Its Appl. 389 (13), 2607–2616.
Zheng, Z., Ahn, S., Monsere, C.M., 2010. Impact of traffic oscillations on freeway crash occurrences. Accid. Anal. Prev. 42 (2), 626–636.
Zhu, H.B., Dai, S.Q., 2008. Analysis of car-following model considering driver's physical delay in sensing headway. Phys. A Stat. Mech. Appl. 387 (13), 3290–3298.